PROTEINS: Structure, Function, and Bioinformatics 68:223–231 (2007)

Conformation Transition Kinetics of *Bombyx mori* Silk Protein

Xin Chen,[1,2*] Zhengzhong Shao,[1] David P. Knight,[2] and Fritz Vollrath[2]
[1]*The Key Laboratory of Molecular Engineering of Polymers of MOE, Department of Macromolecular Science, Fudan University, Shanghai 200433, People's Republic of China*
[2]*Department of Zoology, University of Oxford, South Parks Road, Oxford OX1 3PS, United Kingdom*

ABSTRACT **Time-resolved FTIR analysis was used to monitor the conformation transition induced by treating regenerated *Bombyx mori* silk fibroin films and solutions with different concentrations of ethanol. The resulting curves showing the kinetics of the transition for both films and fibroin solutions were influenced by the ethanol concentration. In addition, for silk fibroin solutions the protein concentration also had an effect on the kinetics. At low ethanol concentrations (for example, less than 40% v/v in the case of film), films and fibroin solutions showed a phase in which β-sheets slowly formed at a rate dependent on the ethanol concentration. Reducing the concentration of the fibroin in solutions also slowed the formation of β-sheets. These observations suggest that this phase represents a nucleation step. Such a nucleation phase was not seen in the conformation transition at ethanol concentrations >40% in films or >50% in silk fibroin solutions. Our results indicate that the ethanol-induced conformation transition of silk fibroin in films and solutions is a three-phase process. The first phase is the initiation of β-sheet structure (nucleation), the second is a fast phase of β-sheet growth while the third phase represents a slow perfection of previously formed β-sheet structure. The nucleation step can be very fast or relatively slow, depending on factors that influence protein chain mobility and intermolecular hydrogen bond formation. The findings give support to the previous evidence that natural silk spinning in silkworms is nucleation-dependent, and that silkworms (like spiders) use concentrated silk protein solutions, and careful control of the pH value and metallic ion content of the processing environment to speed up the nucleation step to produce a rapid conformation transition to convert the water soluble spinning dope to a tough solid silk fiber. Proteins 2007;68:223–231.**

Key words: silk fiber; spinning mechanism; time-resolved FTIR; β-sheet; nucleation; fibroin; amyloid protein; silkworm; folding

INTRODUCTION

Natural animal silks, both spider dragline silk and silkworm cocoon silk, are of great interest not only because of their excellent portfolio of mechanical properties but also for their remarkable spinning process that converts water-soluble silk protein, spidroin or silk fibroin, into insoluble solid silk fibers.[1–4] In nature silk, fibers are formed under physiological conditions including ambient temperatures, low hydrostatic pressures, low extrusion rates, low draw down ratios, and without toxic solvents, in sharp contrast to the spinning conditions required for man-made fibers.[5,6] Several attempts have been made to extrude silk artificially from redissolved (regenerated) fibroin or recombinant silk protein analogues, but the resulting fibers have been considerably weaker than the natural fibers.[7–14] Therefore, a more detailed understanding of the way in which spiders or silkworms produce silk may help in designing a successful biomimetic artificial spinning method. The simplest description of the natural spinning process is the conversion of the conformation in concentrated spidroin or fibroin solutions from random coil and/or helix to β-sheet by shearing and/or rapid extensional flow.[15] Although several mechanisms have been proposed for the conformation transition,[3,16–18] the details remain to be elucidated.

Many factors, such as pH[19–25] and metallic ions,[21,24–31] are thought to facilitate the conformation transition. A range of methods have been used to study the transition, including FTIR spectroscopy,[32–34] Raman spectroscopy,[7,35,36] circular dichroism,[37–39] NMR spectroscopy,[33,40,41] X-ray scattering,[37,42,43] rheology,[21,22,27] and fluorescence spectroscopy.[39] Most of the studies reported so far using these methods have yielded static rather than dynamic data as they only describe the conformations of silk protein before and after natural spinning or under specified conditions. However, it would be useful to be able to follow protein conformational changes continuously in time while they are induced by various fac-

Grant sponsor: National Natural Science Foundation of China; Grant numbers: 50373006, 20434010; Grant sponsor: Science and Technology Development Foundation of Shanghai; Grant numbers: 05JC14009.

*Correspondence to: Xin (Terry) Chen, Department of Macromolecular Science, Fudan University, Shanghai, 200433, People's Republic of China. E-mail: chenx@fudan.edu.cn

Received 19 September 2006; Revised 15 November 2006; Accepted 29 December 2006

Published online 13 April 2007 in Wiley InterScience (www.interscience.wiley.com). DOI: 10.1002/prot.21414

tors, such as shear force, pH, metallic ions, temperature change, low dielectric constant solvents, etc. This would yield important data about the kinetics of the conformation transition unobtainable by static experiments, leading to a detailed understanding of the sequence of events occurring as random coil and/or helix conformation changes to β-sheet in silk proteins.

FTIR spectroscopy provides a powerful way of examining protein secondary structure while time-resolved FTIR spectroscopy enables the kinetics of conformational transition to be studied.[44] In previous work, we used the latter method to provide dynamic data on the conformational transition process induced by potassium ions in dried *Nephila* spidroin films.[29] Two-dimensional (2D) correlation spectroscopy strengthened this analysis,[45] enabling us to propose a novel, detailed model for the processes involved in the formation of the silk nanofibril. We also used time-resolved FTIR to study the conformation transition induced by ethanol in dried films of regenerated *Bombyx mori* silk fibroin (RSF).[44] As we only used concentrated (70%) ethanol in the latter paper to induce the conformation transition and only applied this to dried fibroin films, we extend our analysis in the current paper to include the effects of more dilute ethanol solutions on fibroin films and on different dilutions of regenerated fibroin dissolved in D_2O. Slowing the conformation transition in these two ways has enabled us to detect a slow nucleation process missed as it occurred too fast with the 70% ethanol and fibroin films we used in our previous study. The results presented here provide the first evidence that the conformation transition of silk fibroin is a three-phase process.

MATERIALS AND METHODS

Preparation of RSF Film and Solution

Raw silk consists of fibroin fibers that are bound together by several hydrophilic gum-like coat proteins, the sericin. To avoid the possible complication of the these hydrophilic proteins on the conformation transition, we removed them by thoroughly degumming raw silk by boiling it for two 30 min changes of 0.5% (w/w) $NaHCO_3$ solution. After exhaustive washing in distilled water the degummed fibers were allowed to air dry at room temperature.

Dry degummed silk fibers were dissolved in 9.5 mol/L LiBr aqueous solution according to established procedures.[29,44] After dialysis against pure water for 3 days at room temperature, the solution was lightly centrifuged to give a clear supernatant. The concentration of RSF solution was about 1.0% (w/w). To prepare films, 1 mL of RSF solution was transferred to a 3×3 cm^2 polystyrene weighing boat and allowed to dry overnight at ~25°C and 50% relative humidity. The thickness of the film was about 5 μm.

To prepare fibroin solutions, three freshly prepared RSF films were dissolved in 2 mL heavy water (D_2O, from Sigma). The RSF D_2O solution (shortened to "RSF solution" in the text) was obtained by lightly centrifuging to remove traces of undissolved RSF. We used D_2O to dissolve RSF and to prepare ethanol solutions (see later) for the following reasons: a resonance band of light water (H_2O) overlaps the amide I resonance used for the study of the conformation transition, preventing its use as a solvent for this purpose[46]; our previous evidence indicated that D_2O does not appear to have a marked affect on β-sheet.[29,31,44] The concentration of as-prepared RSF solution was about 2.0% (w/w) determined by weighing after exhaustive drying. As the concentration of the as-prepared solution varied a little from batch to batch, the final stock RSF solution was made up to the concentration of 1.8% (w/w) each time by adding appropriate volumes of D_2O. The highest concentration of RSF that can be dissolved in D_2O is about 2.0% (w/w), enough for FTIR measurements, even after diluting with ethanol.

Time-Resolved FTIR Measurement

All infrared spectra were recorded using a Nicolet Nexus 470 FTIR spectrometer. To eliminate spectral contributions due to atmospheric water vapor, the instrument was continuously purged with pure nitrogen gas. The infrared spectra were recorded using a liquid nitrogen cooled MCT detector. For each measurement, 64 interferograms were co-added and Fourier-transformed employing a Genzel-Happ apodization function to yield spectra with a nominal resolution of 4 cm^{-1}.

The RSF films were cut into 8×15 mm^2 rectangles. For the time-resolved measurements, the RSF film was placed between a pair of BaF_2 windows separated by a 100 μm spacer in a liquid cell. The ethanol D_2O solutions (shortened to "ethanol solution" in the text) with concentrations ranging from 10% (v/v) to 99.7% (commercial absolute ethanol without further treatment) were quickly injected into the liquid cell and the gathering of spectra was immediately initiated. Because of the parameter chosen earlier (64 scans per spectrum and the resolution of 4 cm^{-1}), the interval between two successive spectra in the "rapid scan" mode was 9.1785 s (0.153 min); therefore, the time between the injection of ethanol solution and the start of spectra recording was also set at ~9 s (one spectrum interval). The total data collection time was 60 min for each measurement.

For the time-resolved FTIR measurements of RSF solutions, the RSF stock solution (with a concentration of 1.8%) was mixed with absolute ethanol and D_2O in tubes to make a series RSF of solutions (with final RSF concentrations ranging from 0.36 to 0.90% and final ethanol concentrations from 40 to 70%). After mixing, the resulting solution was transferred to the liquid cell described earlier. Mixing took about 45 s and loading into the cell about 15 s. The total time from the solution mixing to the start of spectra recording was precisely controlled to 60 s. Other parameters in the time-resolved measurements were the same as those for RSF films.

Absorbance spectra at each time point were generated by dividing the single beam spectrum collected at a specific time by a background spectrum and converting to

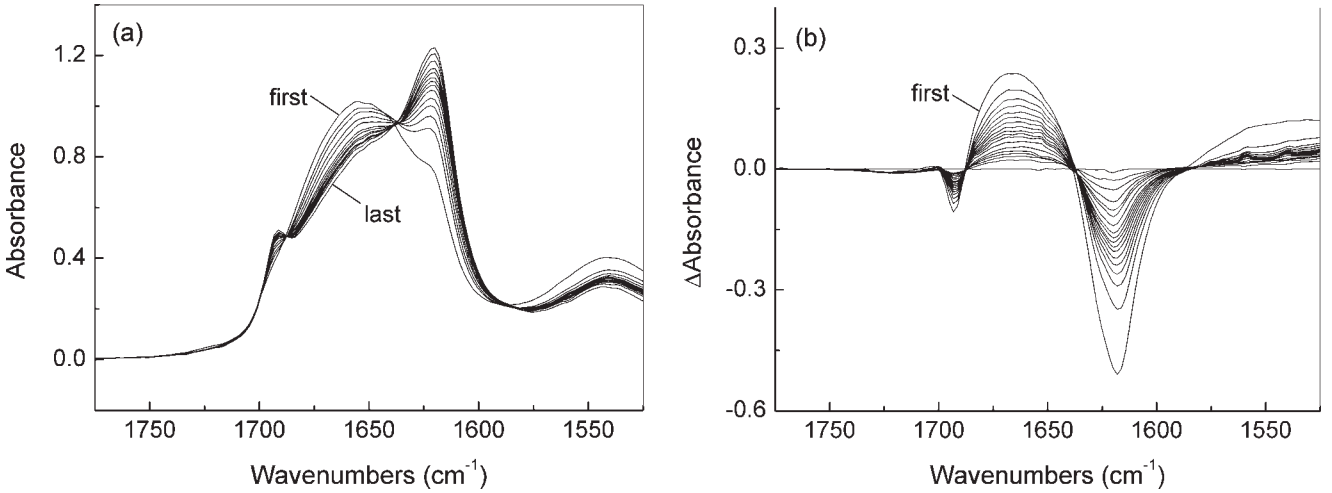

Fig. 1. Original FTIR spectra (**a**) and difference spectra (**b**) of RSF film during the conformation transition process from 9 s to 60 min after the addition of 60% ethanol.

absorbance using OMNIC 5.1 (Microcal). The difference spectra were calculated by the subtraction of an absorbance spectrum collected at 60 min from each absorbance spectrum at time t after the addition of ethanol. The data shown in the figures are from single experiments, but closely similar results were obtained in replicates. Peak separation of amide I band was carried out using PeakFit 4.1 (SPSS Inc.). As in our previous studies, a Gaussian model was selected for the band shape; the band position was set at 1620, 1652, and 1691 cm^{-1}, which represented β-sheet, random coil and/or helical conformation (shortened to "random coil" in the text), and β-turn associated with β-sheet (shortened to "β-turn" in the text), respectively[29,45]; and the band width was automatically adjusted by the software. The increase of absorbance of the 1620 cm^{-1} band was used as a probe for the β-sheet formation during the conformation transition process as in our previous work. Kinetics of the ethanol-induced conformation transition was studied by fitting curves using Origin 7.0 (OriginLab Corporation). All data reported in the text were the means and standard deviations for at least three separate runs.

RESULTS AND DISCUSSION

Time-Resolved FTIR Analysis of RSF Films

We found that ethanol solutions only between 20 and 93% can induce a conformation transition in RSF films. The RSF films dissolved in ethanol solution when the concentration was lower than 20%. The reason for the lack of conformation transition at ethanol concentration higher than 93% is thought to be the insufficient swelling of RSF films in solutions containing little water.[47]

Figure 1 shows the time-resolved FTIR spectra and the related difference spectra of a RSF film treated with 60% ethanol. They clearly show the development of the absorption bands at 1620, 1652, and 1691 cm^{-1} corresponding to β-sheet, random coil, and β-turn, respectively. The assignments of these bands is discussed in our previous papers and the literature referred to therein.[29,44] The plots in Figure 1 are closely similar to those for the conformation transition induced by 70% ethanol.[44]

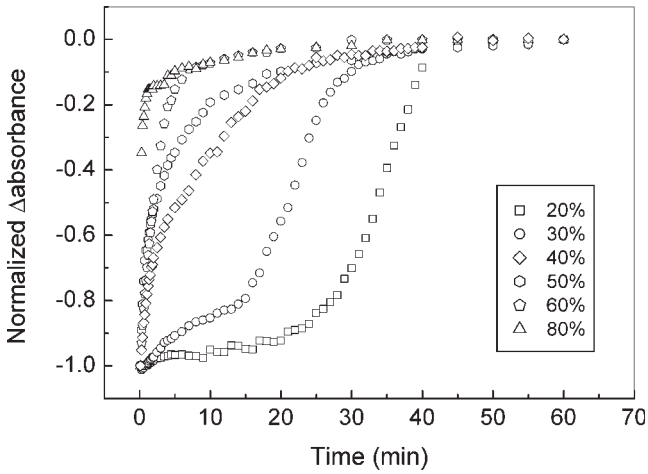

Fig. 2. Normalized Δ absorbance–time curves at 1620 cm^{-1} for the RSF films showing the effect of different concentrations of ethanol on the kinetics of β-sheet formation.

Figure 2 shows the effect of different concentrations of ethanol on the normalized Δabsorbance–time curves at 1620 cm^{-1} of the RSF films to compare the kinetics of β-sheet formation under these conditions. The curve for 80% ethanol was very close to that for 70% as previously reported,[44] showing an immediate sharp increase indicating very rapid formation β-sheet under these conditions. Figure 2 shows that with a decrease in ethanol concentration there was a progressive slowing in β-sheet formation. This was accompanied by marked changes in the shape of the Δabsorbance–time curves at ethanol concentrations beneath about 40% as the curves became

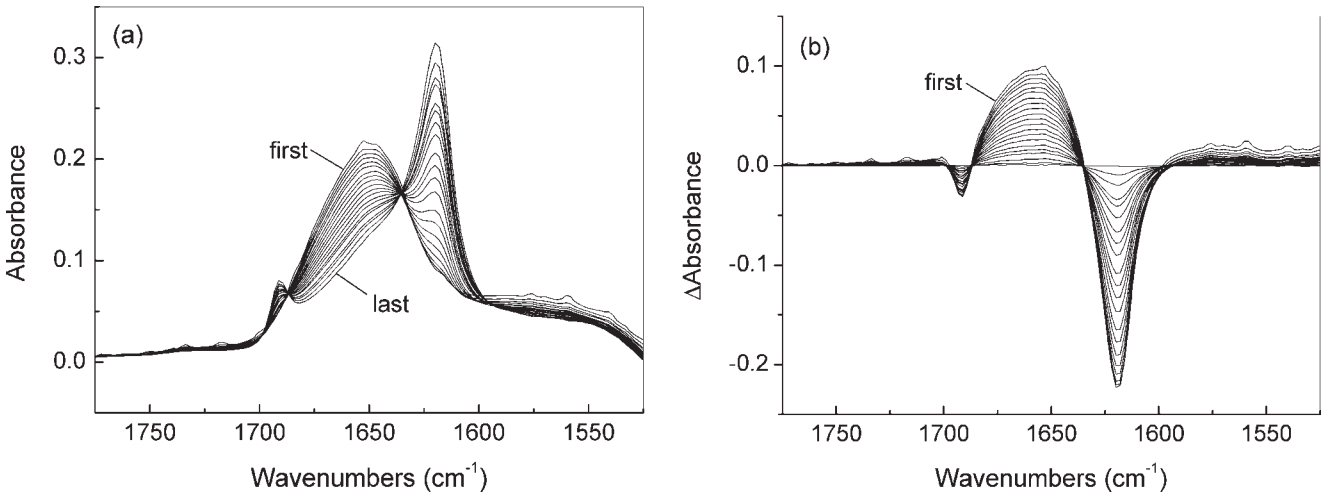

Fig. 3. Original FTIR spectra (**a**) and difference spectra (**b**) of RSF solution during the conformation transition process from 1.0 to 60 min after mixing with ethanol. Final concentrations: ethanol 50%; silk fibroin 0.72% (w/w).

S-shaped. Thus, three phases in the conformation transition can be clearly resolved at low ethanol concentrations. A lag phase in which β-sheet formation occurs slowly, a phase of rapid β-sheet formation, and a third phase of slowing β-sheet formation. In our previous FTIR spectroscopic studies,[29,44] we proposed a two-phase mechanism for the conformation transition in silk fibroin, assuming a rapid phase for adjusting individual protein segments and a slowing phase for rearrangement of whole macromolecular chains. We missed the lag phase clearly seen in the present study at low ethanol concentrations because it occurred too fast to be detected in the 70% ethanol previously used. Thus the curves in Figure 2 show that the lag phase occurs before the previously detected fast phase and that the rate constant of the newly detected lag phase is highly dependent on the ethanol concentration. The lag phase of β-sheet formation is rather protracted at low ethanol concentrations, lasting about 25 min for 20% ethanol and about 15 min for 30% ethanol. No β-sheet formation was detected within the 60 min observation period when the ethanol was lower than 20% and the films dissolved probably because of the failure of intermolecular β-sheet formation.

The kinetic curves of β-sheet formation for ethanol concentrations >40% showed a good fit with a biphasic exponential decay function. The time constants of the fast phase (τ_1) were 1.73, 1.18, 0.63, and 0.41 min when induced by 50, 60, 70, and 80% ethanol solution, respectively. The large increase in Δabsorbance during this phase in which segment adjustment is thought to occur indicates that this phase accounts for most of the β-sheet formation. From the kinetic curves and the value of τ_1, the most rapid β-sheet formation in RSF film occurs when ethanol concentration is about 70–80%, the τ_1 increasing again (to 1.9 min) for 90% ethanol[47] and occurring too slowly to be detected at ethanol concentrations ≥93%. The slowing of β-sheet formation at ethanol concentration >80% presumably results from the reduction in water content giving insufficient swelling of the film to permit the chain mobility required for chain rearrangement.[47]

A more detailed examination of the Δabsorbance–time curves in Figure 2 show that while the kinetic curves for 20 and 30% ethanol are approximately S-shaped they do show a slight but significant initial inflection at about 5–10 min, while a slight apparent change in slope in curve for 40% ethanol at this time may be significant. This inflection may represent an initial component of the lag phase with different kinetics perhaps representing the first formation within the molecules of small numbers β-sheets, which later propagate along the molecules in the rest of the lag phase to form the nucleation sights for rapid β-sheet formation.

Time-Resolved FTIR Analysis of RSF D_2O Solutions

The time-resolved FTIR spectra and the related difference spectra of RSF solution treated with 50% ethanol (see Fig. 3) are similar to those of RSF films but show more marked changes with time. For ease of interpretation, Figure 4 shows the same series of time-resolved FTIR spectra shown in Figure 3 but plotted in three-dimensions (3D). Ethanol produces a much more marked increase in the β-sheet band (1620 cm^{-1}) in solutions than in films (compare Fig. 3 with Fig. 1). This may imply that β-sheet structure forms more readily in the solution because the protein chains can move and adjust more freely and completely than in the films.

At low alcohol concentrations (<40%), the transition occurred too slowly to be observed within the 60 min period we used for FTIR. In contrast, at high concentrations (>70%) gelation occurred in less than 1 min and β-sheet formation was substantially complete within 10 min. Both original and normalized Δabsorbance–time curves at 1620 cm^{-1} (see Fig. 5) are presented for RSF solutions to show the effect of ethanol concentration

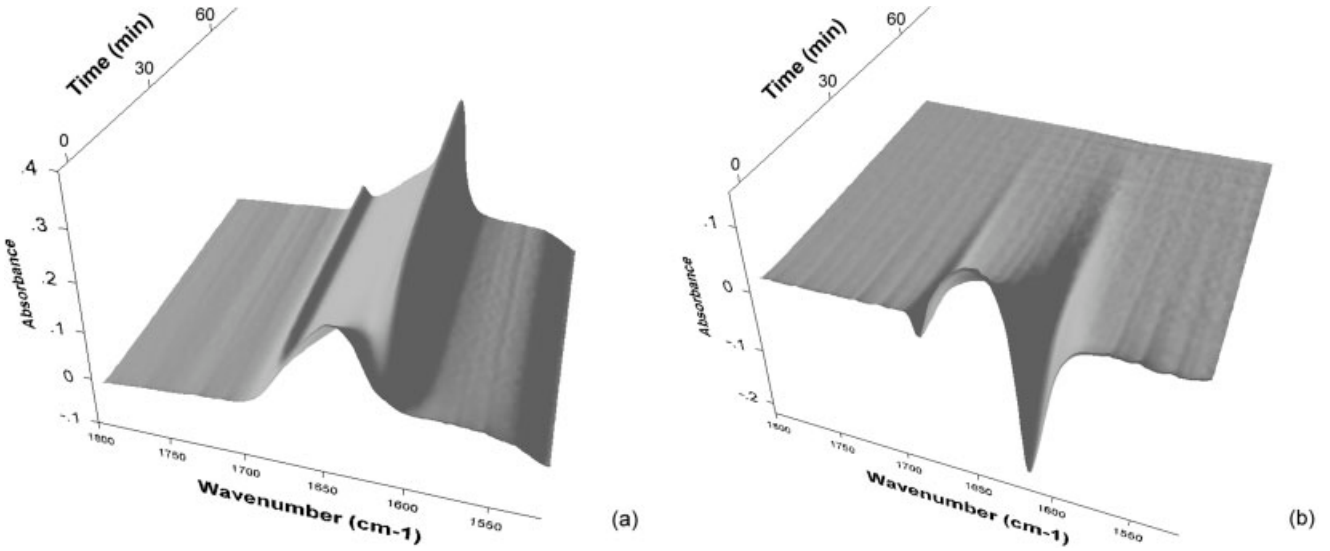

Fig. 4. 3D plots of the original (**a**) and difference (**b**) spectra presented in Figure 3.

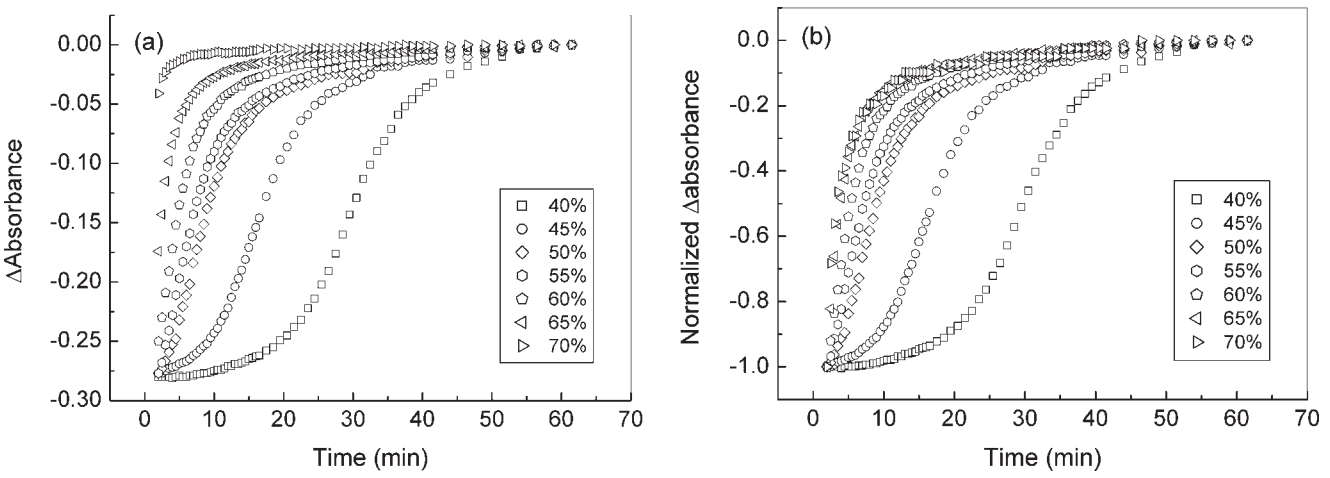

Fig. 5. Original (**a**) and normalized (**b**) Δ absorbance–time curves at 1620 cm^{-1} for 0.72% (w/w) RSF solutions showing the effect of different concentrations of ethanol on the kinetics of β-sheet formation.

on the kinetics of β-sheet formation. In contrast, only normalized Δabsorbance–time curves could be presented for RSF films as a consequence of variations in film thickness.

As in RSF films, RSF solutions show a progressive increase in the rate of β-sheet formation with increase in ethanol concentration over the range used. The original Δabsorbance–time curves for RSF solutions [Fig. 5(a)] enable a direct comparison of the effect of ethanol on the conformation transition rates. For example, β-sheet formation in RSF solutions is substantially complete within 1 min in 70% ethanol solution, but takes ~10 min in 60%, 25 min in 45%, and 40 min in 40% ethanol, to form the same proportion of β-sheet. The normalized Δabsorbance–time curves of RSF solutions [Fig. 5(b)] were approximately similar to those of RSF films (Fig. 2). At ethanol concentration of 40 or 45%, the kinetic curves of RSF solution show a clear S-shape as in RSF films in 20–30% ethanol with no evidence of the slight initial inflection. The absence of this inflection in RSF solutions may result from the faster kinetics of the lag phase in RSF solution, lasting about 10 min for 45% and about 25 min for 40% ethanol.

The kinetic curves of β-sheet formation in 55–70% ethanol (Fig. 5) showed a good fit with biphasic exponential decay function while the curve for 50% showed a very short lag phase. The time constants of the fast phase (τ_1) and slow phase (τ_2) (Table I) decrease with the increase of ethanol concentration as in RSF films.

In addition to studying the effects of varying the ethanol concentration on silk fibroin solutions, we also studied the effect of varying RSF concentration on the conformation transition kinetics at a single ethanol concentration. We chose 50% ethanol solution and a range of RSF concentration from 0.36 to 0.90%. The kinetic curves in Figure 6 show that increasing the fibroin con-

TABLE I. Conformation Transition Kinetics for 0.72% RSF Solution Determined by Fitting a Biphasic Exponential Decay Function to ΔAbsorbance–Time Curves at 1620 cm^{-1}

Time constant	50% ethanol	55% ethanol	60% ethanol	65% ethanol	70% ethanol
τ_1 (min)	7.3 ± 1.1	5.2 ± 0.1	2.6 ± 1.0	2.4 ± 0.6	1.1 ± 0.2
τ_2 (min)	36.7 ± 9.0	22.8 ± 0.5	16.1 ± 3.2	15.4 ± 1.9	12.8 ± 2.5

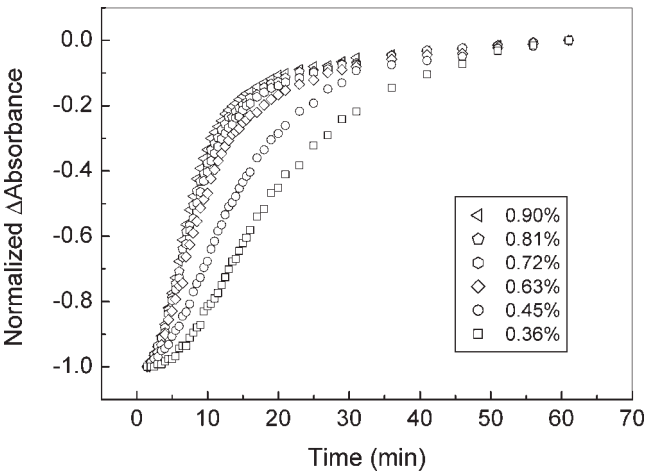

Fig. 6. Normalized Δ absorbance–time curves at 1620 cm^{-1} showing the effects on the kinetics of β-sheet formation produced by varying the silk fibroin concentration but maintaining the ethanol concentration at 50%.

centration increased the rate of the formation of β-sheet. While curves for RSF concentrations ≤0.63% cannot be fitted with a biphasic exponential decay function, those >0.63% give a good fit. This indicates the existence at low RSF concentrations of the lag phase described earlier in RSF films treated with low concentrations of ethanol.

The Mechanism of the Conformation Transition in Silk Proteins

In our previous study,[44] we proposed a two-phase conformation transition mechanism of *B. mori* silk fibroin based on the study of RSF films induced by 70% ethanol solution. We confirmed the existence of a two-phase conformation transition in *Nephila* spidroin films induced by potassium chloride[29] and other metal chlorides.[31] However, in those cases, the conformation took place very fast, and so the "burst phase" for the formation of β-sheet already existed in the first spectra recorded in FTIR time series. Though we missed kinetic data within the first 9 s, we can compare the β-sheet formation rate by comparing the β-sheet contents in the first spectra. In our previous study we roughly estimated that half of the β-sheet structure had been formed in the burst phase when induced by 70% ethanol.[44] In the present study, to obtain relatively accurate data for a more detailed analysis of the secondary structural changes occurring in the conformation transition, we used a deconvolution technique to separate amide I band into three components corresponding to random coil, β-sheet, and β-turn (see Experimental section) and estimate the percentage of each conformation. For ethanol concentration from 60–85%, we found that β-sheet already existed in the first spectrum for RSF films [Fig. 7(a)]. Films treated with 70–80% ethanol had the highest β-sheet content (about 19%), indicating that the conformation transition occurred quickest in this range of ethanol concentrations.

Previous work has shown that the conformation transition of silk protein from random coil to β-sheet is due to the rearrangement of the hydrogen bonds between the polypeptide chains, and the transition may be a nucleation-dependent aggregation.[48] In the case of RSF film induced by ethanol solution, the more water in the solution (lower concentration), the easier it is for the film to swell and hence for the molecular chains to move. When the water content in ethanol solution is low ([EtOH] > 93%), the film is only slightly swollen, and so the movement of the silk fibroin chains is limited, and consequently no conformation transition occurs within the time period studied.[47] On the other hand, when the water content is too high ([EtOH] < 20%), the hydrogen bonds stabilizing the film are totally destroyed while sufficient water molecules bind to the hydrophilic groups in the individual polypeptide chains to bring them into solution. These two prevent the conformation transition. Therefore, the conformation transition takes place only in certain concentration range, i.e., 93% < [EtOH] < 20% as shown previously. The rate of the conformation transition in RSF films depends on competition between the breaking down of the original hydrogen bonds and the building up of the new ones between the silk fibroin chains. At relatively high ethanol concentration (for instance, 70–80%), the polypeptide chain can move but not very freely, and so both nucleation and the growth step of β-sheet occur readily and rapidly by adjusting the segments of individual chains. With a decrease in ethanol concentration, the original hydrogen bonds are easier to break and the polypeptide chains move more freely, both making the formation of new hydrogen bonds more difficult. This influences the nucleation process more strongly than the burst phase as we find a long slow phase at relative low ethanol concentration (20% < [EtOH] < 30%, see Fig. 2). In summary, the conformation transition rate is thought to depend on the rearrangement of hydrogen bonds between silk fibroin chains controlled by the ethanol concentration so that RSF films in 70% ethanol solution showed the fastest transition rate and gave the highest β-sheet content (33% β-sheet content within 60 min observation period).

The small differences in kinetics suggest that the ethanol induced conformation transition in RSF solu-

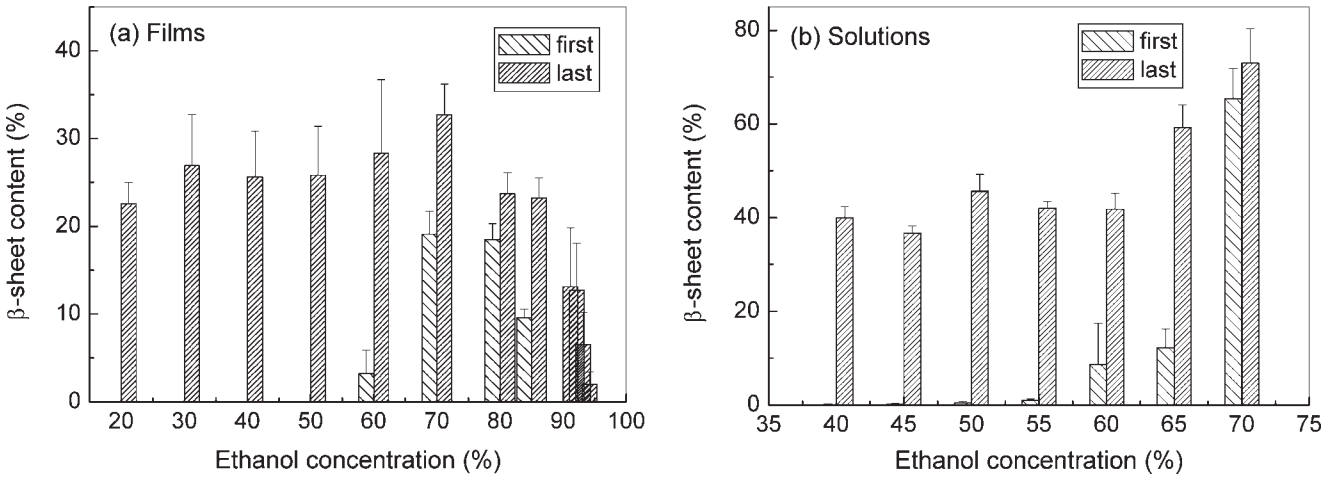

Fig. 7. β-sheet content in the first and last spectrum by time-resolved FTIR analysis of (**a**) RSF film and (**b**) solution (0.72%) induced by different ethanol concentrations.

tions is somewhat different to that in the films. The driving force for nucleation for fibroin in solution appears to be mainly the formation of intermolecular hydrogen bonds. The more concentrated the ethanol solution is, the greater its ability to strip off the bound water surrounding silk fibroin chains and hence the β-sheet nuclei will form faster. This accounts for the observation that in RSF solutions (in contrast to films) the conformation transition rate increases continuously with the increase in ethanol concentration. This is clearly seen in the β-sheet contents after 1 min (the first spectrum in Fig. 7b) and in the kinetic curves (see Fig. 5). In the case of 70% ethanol, the β-sheet formation in solutions was extremely quick, the β-sheet content accounting within 1 min for 65% of all conformations compared with 73% β-sheet of all conformations after 60 min. Thus under these conditions the solutions remarkably after only 1 min already contained 90% of the β-sheet structure present at the end of the 60 min experimental period. Decreasing the ethanol and silk fibroin concentrations in the solution makes it more difficult to nucleate as a result of reduced ability to strip off the water shell and reduced chances for the molecular chains to contact each other. Thus, a slow nucleation phase (lag phase) can be seen (Figs. 5 and 6). A further decrease in [EtOH] <40% (for [RSF] = 0.72%) slows the lag phase while a further decrease in [RSF] <0.36% (for [EtOH] = 50%) evidently extends it so much that no conformation transition is seen within 60 min.

Evidently, the silk fibroin chains move more freely in RSF solution than in the film even in a swollen state, and so the conformation transition from random coil to β-sheet occurs more completely in the solution at given alcohol concentrations. Thus for 70% ethanol, films show only 33% β-sheet content at the end of 60 min while solutions ([RSF] = 0.72%) show 73% β-sheet (see Fig. 7).

According to the evidence shown and the earlier discussion, we propose a hypothetical conceptual model for the conformation transition mechanism of silk proteins as follows. Before the onset of β-sheet formation the silk fibroin molecule has a lamellar hairpin structure as reviewed elsewhere.[45] β-sheet formation occurs in three phases. In phase 1, the lag or nucleation phase, there is a formation of initially isolated intramolecular β-sheets between two anti-parallel strands within the lamellar hairpin structure. These isolated β-sheets lower the energy barrier for the formation of subsequent ones in adjacent chains, resulting in lateral propagation within single lamellae and longitudinal propagation from lamella to lamella along the molecule. β-sheet formation also starts to propagate laterally from molecule to molecule, leading to the formation of nanofibrils stabilized by hydrogen bonding. This nucleation results in an exponential growth in the number of β-sheets but only accounts for small fraction of the total β-sheet formation. As this step involves intermolecular interaction, its rate is highly dependent on fibroin concentration. The exponential rate of growth in the number of β-sheets continues in phase 2, a rapid burst phase in which the bulk of β-sheet is formed. In this phase β-sheet conformation propagates between and along the fibroin molecules. This phase may be less protein concentration dependent than phase 1 because much of the molecular aggregation may be completed in the nucleation phase. However, like phase 1 it will be highly dependent on ethanol concentration or any other factor that helps to strip away the protective water shell around the molecules. Phase 3, the slowing phase only accounts for a small fraction of the total β-sheet formation. It is thought to represent a perfection of existing β-sheets resulting from a slow chain or segment realignment to form more energetically stable β-sheets. This part of the process is likely to be less sensitive to ethanol concentration than the rapid burst phase (see Table I) because it is less dependent on removal of the protective water shell. It is of interest that a recent molecular dynamics simulation of a short model polyalanine peptide known to form amyloid-like β-sheet-stabilized nanofibrils[49] showed three stage kinetics for β-sheet formation similar but much faster than those we observed in

silk fibroin. It revealed that fibril formation was nucleation dependent after a lag phase that shortened with increasing peptide concentration as in our study. The simulation[49] further revealed a conformation conversion process with the following steps: small amorphous aggregates → β-sheets → ordered nuclei → subsequent rapid burst phase forming a small stable fibril or protofilament similar but not identical to that proposed earlier. The greatly larger molecular weight of silk fibroin compared with short amyloid-like peptides probably accounts for its much slower kinetics, the formation of β-sheets parallel to the axis of the fibril in place of the cross-β-structure and differences in detail of the assembly process.

CONCLUSIONS

We present above the kinetic data of RSF films induced by ethanol solution with different concentration that considerably extend our previous study of the conformation transition. In addition, we were able to prepare RSF solutions in D_2O solution enabling us to investigate by FTIR the conformation transition process in solution and the effect of protein concentration for the first time. According to the kinetic data obtained by time-resolved FTIR spectroscopy, both from RSF films and solutions, we modify our understanding of the conformation transition for silk fibroin from a two-phase to a three-phase mechanism. Our evidence suggests that the initiation of β-sheet structure (nucleation) occurs in the first phase while the second phase corresponds to the rapid growth of β-sheet structure. A perfection of the β-sheet structure is thought to take place in the third phase. Our observation from the conformation transition kinetics of silk protein is compatible with the suggestion that the natural silk spinning process may follow a nucleation-dependent aggregation mechanism.[48] In addition, our observation may help to explain why both silkworms and spiders use high concentrated silk protein solution (approximately 26% for silkworm[50] and 34% for spider[21]) as spinning dope to balance freedom of chain movement with ease of intermolecular hydrogen bond formation. Our observations may also help to explain why both organisms reduce the pH[21,22] and add metallic ions[20,50] during the spinning process as these speed up the nucleation process to achieve a sufficiently rapid conformation transition to convert the water soluble spinning dope to a tough solid silk fiber. Finally we note that the remarkably slow kinetics of silk fibroin solutions under certain conditions and the ability to obtain large quantities of this protein make it an ideal model system for studying the detailed mechanism of protein folding and aggregation in a β-sheet protein with possible relevance to the study of these processes in the disease-causing amyloids, neurofibrillary, and prion proteins.

ACKNOWLEDGMENTS

We thank Miss Rong Zeng and Miss Wen Zhou for their hard work to process the experimental data.

REFERENCES

1. Gosline JM, DeMont ME, Denny MW. The structure and properties of spider silk. Endeavour 1986;10:31–43.
2. Hinman MB, Jones JA, Lewis RV. Synthetic spider silk: a modular fiber. Trends Biotechnol 2000;18:374–379.
3. Vollrath F, Knight DP. Liquid crystalline spinning of spider silk. Nature 2001;410:541–548.
4. Yang Y, Chen X, Shao ZZ, Zhou P, Porter D, Knight DP, Vollrath F. Toughness of spider silk at high and low temperatures. Adv Mater 2005;17:84–88.
5. Viney C, Huber AE, Dunaway DL, Kerkam K, Case ST. Optical characterization of silk secretions and fibers. In: Kaplan D, Adams WW, Farmer B, Viney C, editors. Silk polymers. Washington: American Chemical Society; 1994. pp 120–136.
6. Shao ZZ, Vollrath F. Materials: surprising strength of silkworm silk. Nature 2002;418:741–741.
7. Trabbic KA, Yager P. Comparative structural characterization of naturally- and synthetically-spun fibers of *Bombyx mori* fibroin. Macromolecules 1998;31:462–471.
8. Seidel A, Liivak O, Jelinski LW. Artificial spinning of spider silk. Macromolecules 1998;31:6733–6736.
9. Seidel A, Liivak O, Calve S, Adaska J, Ji GD, Yang ZT, Grubb D, Zax DB, Jelinski LW. Regenerated spider silk: processing, properties, and structure. Macromolecules 2000;33:775–780.
10. Liivak O, Blye A, Shah N, Jelinski LW. A microfabricated wet-spinning apparatus to spin fibers of silk proteins. Structure-property correlations. Macromolecules 1998;31:2947–2951.
11. Yao J, Masuda H, Zhao C, Asakura T. Artificial spinning and characterization of silk fibre from *Bombyx mori* silk fibroin in hexafluoroacetone hydrate. Macromolecules 2002;35:6–9.
12. Arcidiacono S, Mello CM, Butler M, Welsh E, Soares JW, Allen A, Ziegler D, Laue T, Chase S. Aqueous processing and fiber spinning of recombinant spider silks. Macromolecules 2002;35:1262–1266.
13. Lazaris A, Arcidiacono S, Huang Y, Zhou JF, Duguay F, Chretien N, Welsh EA, Soares JW, Karatzas CN. Spider silk fibers spun from soluble recombinant silk produced in mammalian cells. Science 2002;295:472–476.
14. Lock RL. Process for making silk fibroin fibers. US Patent 5,252,285; 1993.
15. Winkler S, Kaplan DL. Molecular biology of spider silk. Rev Mol Biotechnol 2000;74:85–93.
16. Jin HJ, Kaplan DL. Mechanism of silk processing in insects and spiders. Nature 2003;424:1057–1061.
17. Willcox PJ, Gido SP, Muller W, Kaplan DL. Evidence of a cholesteric liquid crystalline phase in natural silk spinning processes. Macromolecules 1996;29:5106–5110.
18. Kenney JM, Knight D, Wise MJ, Vollrath F. Amyloidogenic nature of spider silk. Eur J Biochem 2002;269:4159–4163.
19. Magoshi J, Magoshi Y, Nakamura S. Mechanism of fiber formation of silkworm. In: Kaplan D, Adams WW, Farmer B, Viney C, editors. Silk polymers. Washington: American Chemical Society; 1994. pp 292–310.
20. Knight DP, Vollrath F. Changes in element composition along the spinning duct in a *Nephila spider*. Naturwissenschaften 2001;88:179–182.
21. Chen X, Knight DP, Vollrath F. Rheological characterization of *Nephila spidroin* solution. Biomacromolecules 2002;3:644–648.
22. Terry AE, Knight DP, Porter D, Vollrath F. pH induced changes in the rheology of silk fibroin solution from the middle division of *Bombyx mori* silkworm. Biomacromolecules 2004;5:768–772.
23. Dicko C, Vollrath F, Kenney JM. Spider silk protein refolding is controlled by changing pH. Biomacromolecules 2004;5:704–710.
24. Zong XH, Zhou P, Shao ZZ, Chen SM, Chen X, Hu BW, Deng F, Yao WH. Effect of pH and copper(II) on the conformation transitions of silk fibroin based on EPR, NMR, and Raman spectroscopy. Biochemistry 2004;43:11932–11941.
25. Dicko C, Kenney JM, Knight D, Vollrath F. Transition to a beta-sheet-rich structure in spidroin in vitro: the effects of pH and cations. Biochemistry 2004;43:14080–14087.
26. Magoshi J. Biospinning (silk fiber formation, multiple spinning mechanisms). In: Salamone JC, editor. Polymeric materials encyclopedia. New York: CRC Press; 1996. pp 667–679.
27. Ochi A, Hossain KS, Magoshi J, Nemoto N. Rheology and dynamic light scattering of silk fibroin solution extracted from

the middle division of *Bombyx mori* silkworm. Biomacromolecules 2002;3:1187–1196.
28. Hossain KS, Ochi A, Ooyama E, Magoshi J, Nemoto N. Dynamic light scattering of native silk fibroin solution extracted from different parts of the middle division of the silk gland of the *Bombyx mori* silkworm. Biomacromolecules 2003;4:350–359.
29. Chen X, Knight DP, Shao ZZ, Vollrath F. Conformation transition in silk protein films monitored by time-resolved Fourier transform infrared spectroscopy: effect of potassium ions on *Nephila spidroin* films. Biochemistry 2002;41:14944–14950.
30. Zhou L, Chen X, Shao ZZ, Zhou P, Knight DP, Vollrath F. Copper in the silk formation process of *Bombyx mori* silkworm. FEBS Lett 2003;554:337–341.
31. Chen X, Shao ZZ, Knight DP, Vollrath F. Conformation transition of silk protein membranes monitored by time-resolved FTIR spectroscopy: effect of alkali metal ions on *Nephila spidroin* membrane. Acta Chim Sinica 2002;60:2203–2208.
32. Lenormant H. Infra-red spectra and structure of the proteins of the silk glands. Trans Faraday Soc 1956;52:549–553.
33. Hijirida DH, Do KG, Michal C, Wong S, Zax D, Jelinski LW. ^{13}C NMR of *Nephila clavipes* major ampullate silk gland. Biophys J 1996;71:3442–3447.
34. Venyaminov SY, Kalnin NN. Quantitative IR spectrophotometry of peptide compounds in water (H_2O) solutions. II. Amide absorption-bands of polypeptides and fibrous proteins in α-coil, β-coil, and random coil conformations. Biopolymers 1990;30:1259–1271.
35. Rousseau ME, Lefevre T, Beaulieu L, Asakura T, Pezolet M. Study of protein conformation and orientation in silkworm and spider silk fibers using Raman microspectroscopy. Biomacromolecules 2004;5:2247–2257.
36. Shao Z, Vollrath F, Sirichaisit J, Young RJ. Analysis of spider silk in native and supercontracted states using Raman spectroscopy. Polymer 1999;40:2493–2500.
37. Canetti M, Seves A, Secundo F, Vecchio G. CD and small-angle X-ray scattering of silk fibroin in solution. Biopolymers 1989;28:1613–1624.
38. Dicko C, Knight D, Kenney JM, Vollrath F. Structural conformation of spidroin in solution: a synchrotron radiation circular dichroism study. Biomacromolecules 2004;5:758–767.
39. Yang YH, Shao ZZ, Chen X, Zhou P. Optical spectroscopy to investigate the structure of regenerated *Bombyx mori* silk fibroin in solution. Biomacromolecules 2004;5:773–779.
40. Asakura T, Yao JM, Yamane T, Umemura K, Ultrich AS. Heterogeneous structure of silk fibers from *Bombyx mori* resolved by ^{13}C solid-state NMR spectroscopy. J Am Chem Soc 2002; 124:8794–8795.
41. Asakura T, Sugino R, Yao JM, Takashima H, Kishore R. Comparative structure analysis of tyrosine and valine residues in unprocessed silk fibroin (silk I) and in the processed silk fiber (silk II) from *Bombyx mori* using solid-state ^{13}C, ^{15}N, and ^{2}H NMR. Biochemistry 2002;41:4415–4424.
42. Riekel C, Muller M, Vollrath F. In situ X-ray diffraction during forced silking of spider silk. Macromolecules 1999;32:4464–4466.
43. Riekel C, Madsen B, Knight D, Vollrath F. X-ray diffraction on spider silk during controlled extrusion under a synchrotron radiation X-ray beam. Biomacromolecules 2000;1:622–626.
44. Chen X, Shao ZZ, Marinkovic NS, Miller LM, Zhou P, Chance MR. Conformation transition kinetics of regenerated *Bombyx mori* silk fibroin membrane monitored by time-resolved FTIR spectroscopy. Biophys Chem 2001;89:25–34.
45. Peng XN, Shao ZZ, Chen X, Knight DP, Wu PY, Vollrath F. Further investigation on potassium-induced conformation transition of *Nephila spidroin* film with two-dimensional infrared correlation spectroscopy. Biomacromolecules 2005;6:302–308.
46. Zuber H, Zahn H. Elektronenmikroskopische Untersuchungen an chemisch modifizierter und beschwerter Naturseide. Melliand Textilberichte 1956;37:429–432.
47. Chen X, Zhou L, Shao ZZ, Zhou P, Knight DP, Vollrath F. Conformation transition of silk protein membranes monitored by time-resolved FT-IR spectroscopy—Conformation transition behavior of regenerated silk fibroin membranes in alcohol solution at high concentrations. Acta Chim Sinica 2003;61:625–629.
48. Morozova-Roche LA, Zamotin V, Malisauskas M, Ohman A, Chertkova R, Lavrikova MA, Kostanyan IA, Dolgikh DA, Kirpichnikov MP. Fibrillation of carrier protein albebetin and its biologically active constructs. Multiple oligomeric intermediates and pathways. Biochemistry 2004;43:9610–9619.
49. Nguyen HD, Hall CK. Kinetics of fibril formation by polyalanine peptides. J Biol Chem 2005;280:9074–9082.
50. Zhou L, Chen X, Shao ZZ, Huang YF, Knight DP. Effect of metallic ions on silk formation in the mulberry silkworm, *Bombyx mori*. J Phys Chem B 2005;109:16937–16945.